Molecular Biology of the Cell
Vol. 15, 5197–5207, December 2004

Inhibiting the Arp2/3 Complex Limits Infection of Both Intracellular Mature Vaccinia Virus and Primate Lentiviruses

Jun Komano,* Kosuke Miyauchi, Zene Matsuda, and Naoki Yamamoto

Laboratory of Virology and Pathogenesis, AIDS Research Center, National Institute of Infectious Diseases, Tokyo 208-0011, Japan

Submitted April 2, 2004; Revised September 6, 2004; Accepted September 13, 2004
Monitoring Editor: Thomas Pollard

Characterizing cellular factors involved in the life cycle of human immunodeficiency virus type 1 (HIV-1) is an initial step toward controlling replication of HIV-1. Actin polymerization mediated by the Arp2/3 complex has been found to play a critical role in some pathogens' intracellular motility. We have asked whether this complex also contributes to the viral life cycles including that of HIV-1. We have used both the acidic domains from actin-related protein (Arp) 2/3 complex-binding proteins such as the Wiscott-Aldrich syndrome protein (N-WASP) or cortactin, and siRNA directing toward Arp2 to inhibit viral infection. HIV-1, simian immunodeficiency virus (SIV), and intracellular mature vaccinia virus (IMV) were sensitive to inhibition of the Arp2/3 complex, whereas MLV, HSV-1, and adenovirus were not. Interestingly, pseudotyping HIV-1 with vesicular stomatitis virus G protein (VSV-G) overcame this inhibition. Constitutive inhibition of the Arp2/3 complex in the T-cell line H9 also blocked replication of HIV-1. These data suggested the existence of an Arp2/3 complex-dependent event during the early phase of the life cycles of both primate lentiviruses and IMV. Inhibiting the HIV-1's ability to activate Arp2/3 complex could be a potential chemotherapeutic intervention for acquired immunodeficiency syndrome (AIDS).

INTRODUCTION

When human immunodeficiency virus type 1 (HIV-1) enters cells, the envelope glycoprotein gp120 binds to CD4 and subsequently CXCR4 or CCR5 and initiates membrane fusion at the cell surface. After the membrane fusion the reverse transcription takes place while the viral core components migrate toward cell nucleus where the proviral DNA integrates into the host cell chromosome. However, the protein-protein interactions during these processes of disassembly/uncoating are the least understood among the whole viral life cycle. Despite historical suggestions that actin plays a role in the early phase of HIV-1 infection, its role remains largely unclear. Early studies used chemical inhibitors of actin, which were broadly active on cell physiology or "nonspecific" (Cudmore *et al.*, 1997; Bukrinskaya *et al.*, 1998; Iyengar *et al.*, 1998). To test for a specific role of actin in the early phase of HIV-1's life cycle, we focused on regulators of actin polymerization. It has now been shown that some bacteria and viruses use cellular actin polymerization to propel themselves within cells (Gruenheid and Finlay, 2003). The key host proteins in these reactions are actin-related protein (Arp) 2/3 complex and its regulators. We hypothesized that Arp2/3 complex-dependent actin nucleation might be required for efficient infection by primate lentiviruses including HIV-1.

The Arp2/3 complex is a seven-subunit protein complex highly conserved among eukaryotes that nucleates actin filaments from the sides of existing filaments (Higgs and Pollard, 2001; Pantaloni *et al.*, 2001). The Arp2/3 complex distributes throughout the cell but is enriched especially at the cortical layer underneath the plasma membrane through which viruses have to pass to infect cells (Flanagan *et al.*, 2001). The Arp2/3 complex is regulated by both Wiscott-Aldrich syndrome protein (WASP) family of proteins and cortactin (Weaver *et al.*, 2003). The carboxy terminal domain of WASP is called VCA domain (verprolin homology, cofilin homology and acidic subdomains) and is also named the WA domain. Intensive studies had revealed that VCA's ability to bind monomer actin through its V subdomain is critical for actin nucleation (Miki and Takenawa, 1998). The CA subdomain confers to N-WASP its binding ability to the Arp2/3 complex as evidenced by physicochemical assays (Machesky and Insall, 1998; Marchand *et al.*, 2001) and x-ray crystallography and cross-linking experiments (Gournier *et al.*, 2001; Robinson *et al.*, 2001; Zalevsky *et al.*, 2001). Actin polymerization, nucleation, and branching are enhanced in the presence of VCA protein in vitro (Higgs *et al.*, 1999; Machesky *et al.*, 1999; Rohatgi *et al.*, 1999). Expression of the VCA protein sequesters the Arp2/3 complex and displaces it from physiological regulation in vivo (Machesky and Insall, 1998; Machesky *et al.*, 1999; Rozelle *et al.*, 2000; Castellano *et al.*, 2001; Harlander *et al.*, 2003). By expressing in tissue culture cells, the VCA protein has been used successfully as an inhibitor of Arp2/3 complex to study the role of

Article published online ahead of print. Mol. Biol. Cell 10.1091/mbc.E04–04–0279. Article and publication date are available at www.molbiolcell.org/cgi/doi/10.1091/mbc.E04–04–0279.

* Corresponding author. E-mail address: ajkomano@nih.go.jp.

Abbreviations used: Arp2/3, actin-related protein 2/3; CC, cytochalasin; GFP, green fluorescent protein; HIV-1, human immunodeficiency virus type 1; HSV-1, herpes simplex virus type 1; IMV, intracellular mature virus; MLV, murine leukemia virus; RLU, relative light unit; SIV, simian immunodeficiency virus; VSV-G, vesicular stomatitis virus G protein; VV, vaccinia virus; WASP, Wiscott-Aldrich syndrome protein.

Arp2/3 complex in many biologic processes (Zhang *et al.*, 1999; Krause *et al.*, 2000; May *et al.*, 2000; Moreau *et al.*, 2000; Rozelle *et al.*, 2000; McGee *et al.*, 2001; Zhang *et al.*, 2002).

Another Arp2/3 complex regulator is cortactin, a filamentous actin-associated protein originally identified as a substrate of *Src* (Weed and Parsons, 2001) that is also implicated in the phagocytosis of several invasive bacteria (Dehio *et al.*, 1995; Fawaz *et al.*, 1997; Cantarelli *et al.*, 2000). Cortactin binds directly to the Arp2/3 complex through its amino-terminal acidic domain, NTA, and activates it (Weed *et al.*, 2000; Uruno *et al.*, 2001; Weaver *et al.*, 2001). The NTA protein, like VCA, can serve as an inhibitor of Arp2/3 complex.

We explored the possible involvement of Arp2/3 complex in the early phase of life cycle of primate lentiviruses. In parallel, we tested different virus species including adenovirus, herpes simplex virus type 1 (HSV-1), Moloney murine leukemia virus (MLV), and intracellular mature vaccinia virus (IMV), all of which were reported to use the actin cytoskeleton to infect cells; however, the physical properties and mechanisms of their entry vary (Rosenthal *et al.*, 1985; Kizhatil and Albritton, 1997; Bukrinskaya *et al.*, 1998; Iyengar *et al.*, 1998; Li *et al.*, 1998). We also tested whether changing retroviral envelopes, which forces viruses to enter through different routes, affected the efficiencies of viral entry.

MATERIALS AND METHODS

Cells and Viruses

Human embryonic kidney (HEK) 293 cells and Chinese hamster ovary (CHO)-K1 cells were maintained in Dulbecco's modified Eagle's medium (DMEM, Sigma, St. Louis, MO) supplemented with 10% FBS (Hyclone, Logan, UT), penicillin, and streptomycin (Invitrogen, Carlsbad, CA). H9 cells were maintained in RPMI1640 (Sigma) supplemented with 10% FBS, penicillin, and streptomycin. All the mammalian cell lines were incubated at 37°C in the humidified 5% CO_2 atmosphere. Replication incompetent HIV-1 (HXB2 Δ*vpr*, Δ*rev*, Δ*env*, Δ*nef*) was produced by transfecting the proviral DNA carrying renilla luciferase in place of *nef* open reading frame into 293 T-cells along with the expression plasmid for *env*, *tat*, *rev* and *nef* (pIIIex). When pseudotyping HIV-1, *rev* expressing plasmid and either ecotropic MLV envelope (Ragheb and Anderson, 1994) or vesicular stomatitis virus G (VSV-G) expressing plasmid (Clontech, Palo Alto, CA) were cotransfected with the proviral DNA of HIV-1. HXB2 was used for the replication competent HIV-1. The virus was prepared by transfecting the proviral DNA into 293 T-cells, and the supernatants were collected at 2 d posttransfection. SIV (Δ*nef*) encoding firefly luciferase in place of *nef* open reading frame was created based on the IL-2–carrying molecular clone of SIVmac239 (Gundlach *et al.*, 1997; kindly provided by Dr. K. Mori). SIV was prepared by transfecting the proviral DNA into COS7 cells, and the supernatants were collected. MLV was produced by transfecting pCMMP LacZIRESGFP, pCMMP eGFP (generous gift from Dr. J. Young), pCMMP GFP-VCA, or pQcLIN (Clontech) into 293 cells along with *gag/pol* and either ecotropic, amphotropic *env*, or VSV-G–expressing plasmids (Ragheb and Anderson, 1994). HSV-1 (KOS)Rid1/tk12 encoding beta-galactosidase under the regulation of the immediate early promoter ICP4, vaccinia virus encoding T7 RNA polymerase (vTF7.3), and adenovirus type 5 expressing T7 RNA polymerase were generous gifts from Drs. Spear (Dean *et al.*, 1994), Moss (Fuerst *et al.*, 1986), and Ishii (Aoki *et al.*, 1998), respectively, and were prepared according to the previous publications. Adenovirus, HSV-1 and IMV were titrated by the plaque assay using HEK293 or Hela cells; MLV by counting reporter-positive HEK293 cells after 2 to 3 d postinfection, and HIV-1, VSV-G HIV-1, and SIV by using the indicator cells that expressed beta-galactosidase or GFP upon infection. The p24 concentration of eco HIV-1 was adjusted to that of HIV-1 (~100 ng/ml). The neutralization assay using the antibody 2D5 that inhibits infection of IMV but not that of EEV (Ichihashi and Oie, 1996) revealed that 99.4% of our vaccinia virus preparation contained intracellular mature virus (IMV).

Plasmids

The VCA domain (amino acid 392–505) of N-WASP was amplified by PCR from N-WASP cDNA kindly provided by Dr. Takenawa (Miki *et al.*, 1996) with the following primers: VCA sense 5′-CAATTGCCTTCTGATGGGGACCATCAGG-3′ and 5′-AAGCTTCAGTCTTCCCACTCATCATC-3′. The PCR product was subcloned into pCR4 Blunt TOPO (Invitrogen), sequenced, digested with *Mfe*I and *Eco*RI, and cloned into *Eco*RI site of pEGFP-C2 (Clontech), generating pGFP-VCA. Following two primers, 5′-AGATCTTAGTGGCTGATGGCCAAGAGTC-CACACC-3′ and 5′- CAATTGTCAGTCTTCCCACTCATCATC-3′, were used to amplify the CA domain (amino acid 470–505) of N-WASP. The PCR fragment was cloned into *Bgl*II-*Eco*RI sites of pEGFP-C2, giving rise to pGFP-CA. GFP-A expression plasmid was generated by annealing following two oligonucleotides and cloned it into the *Bgl*II-*Eco*RI sites of pEGFP-C2: 5′-GATCGATGAAGATGAAGATGAA-GATGATGAAGAAGATTTTGAGGATGATGATGAGTGGGAAGACTGA-3′ and 5′-AATTTCAGTCTTCCCACTCATCATCATCCTCAAAATCTTCTTCATCATCT-TCATCTTCATCTTCATC-3′. Following oligonucleotides were annealed and ligated into the *Bgl*II site of pGFP-VCA giving rise to pGFP-VCA*: 5′-GATCTAGATAACT-GATGCGGCCGCCG-3′ and 5′-GATCCGGCGGCCGCATCAGTTATCTA-3′. The NTA domain (amino acid 1–84) of cortactin and Arp2 were amplified by PCR from 293T cDNA with following primers: NTA sense 5′-GGATCCTCGAGATGTG-GAAAGCTTCAGCAGGCCAC-3′, NTA antisense 5′-CAATTGTCAATAGCCAT-GGGAAGCTTTTGGTCC-3′; Arp2 sense 5′-GGATCCTCGAGATGGACAGC-CAGGGCAGGAAGG-3′, Arp2 antisense 5′-CAATTGTTATCGAACAGTCACAC-CAAGTTTC-3′. PCR fragments were cloned into pCR4 Blunt TOPO, and the *Bam*HI-*Mfe*I fragments were cloned into *Bgl*II-*Eco*RI sites of pEGFP-C2, generating pGFP-NTA and pGFP-Arp2. pCMMP GFP-VCA was generated by digesting pC-MMP GFP with *Age* I and *Bam*HI, ligated with *Age* I-*Bam*HI fragment from pGFP-VCA. Transfection efficiencies were measured by phRL/CMV (Promega, Madison, WI) or pHIV-1 LTR-GFP-Luciferase. F10, the ecotropic MLV receptor from rat, expression plasmid was created by digesting pcDNA F10-ecoR (Takase-Yoden and Watanabe, 1999) with *Nae*I followed by the self-ligation. The human nectin 1 alpha (HigR) expression plasmid was generated by inserting *Eco*RI fragment of pEF-BOS human nectin 1 alpha 3xFLAG (Sakisaka *et al.*, 2001) into *Eco*RI site of pcDNA3 (Invitrogen). The *Xho*I-*Not*I fragment of either pBCMGSneoCD4 or pBCMGS-neoCCR5 (a generous gift from Dr. Yamashita) was cloned into *Xho*I-*Not*I sites of pcDNA3 (Invitrogen), generating pCD4 and pCCR5, respectively. The *Sna*BI-*Not*I fragment from pCCR5 was cloned into pMACS4ires (Miltenyi Biotec, Bergisch Gladbach, Germany), generating pCCR5 IRES CD4. The CD4 lacking the cytoplasmic tail was amplified by the following primers: 5′-GGATCCCGGGCCACCATGA-ACCGGGGAGTCCCTTTTAGGC-3′and 5′- GAATTCGTGCCGGCACCTGACA-CAGAAGAAGATGCC-3′. The *Xma*I-*Eco*RI fragment was cloned into the *Age*I-*Eco*RI sites of pEGFP-C2, generating pCD4Δcyt. The T7 RNA polymerase (T7 RNAP) expression plasmid pCMMP T7RNAP IRES GFP was created by inserting *Xma*I-*Eco*RI fragment from pVR1-T7 into *Age*I-*Mfe*I sites of pCMMP IRES GFP (Aoki *et al.*, 1998). The T7RNAP reporter plasmid pTM3Luci was described previously (Aoki *et al.*, 1998). The following pairs of oligonucleotides were annealed and cloned into *Apa*I-*Eco*RI sites of pSilencer 1.0-U6 (Ambion, Austin, TX) to generate siRNA expressing vectors directing against GFP and Arp2: GFP sense 5′-GCTGACCCTGAAGTTC-ATCTTCAAGAGAGATGAACTTCAGGGTCAGCTTTTTT-3′ and GFP antisense 5′-AATTAAAAAAGCTGACCCTGAAGTTCATCTCTCTTGAAGATGAACTTC-AGGGTCAGCGGCC-3′; Arp2 sense 5′-CAGCTTTACTTAGAACGAGTTCAA-GAGACTCGTTCTAAGTAAAGCTGTTTTTT-3′ and Arp2 antisense 5′-AATT-AAAAAACAGCTTTACTTAGAACGAGTCTCTTGAACTCGTTCTAAGTAAA-GCTGGGCC-3′.

Transfection, Magnetic Selection, and Infection

Plasmid DNAs were transfected into cells by using either lipofectamin/lipofectamin plus reagent (Invitrogen) or X-tremeGENE siRNA transfection reagent (Roche Diagnostics, Mannheim, Germany) according to the manufacturer's protocol. The latter reagent, with which the transfection efficiencies reached >90% in 293 cells, was specifically used for preparing samples to carry out Western blot analysis demonstrating the reduction of Arp2 levels. In brief, cells were fed in 48-well plates 1–2 d before transfection. Cells were approximately in 50–60% confluency at transfection. After transfection, cells were trypsinized and plated onto 96-well plates. Transfected cells were magnetically selected by using MACS system directing toward CD4 (Miltenyi Biotec). Cells were infected with viruses of ~0.1–0.5 multiplicity of infection by incubating in the virus-containing culture medium at 37°C for 1–4 h.

Cell-to-cell Fusion Assay

The fusion assay was based on the T7RNAP transcription-dependent reporter assay originally described by Nussbaum *et al.* (1994), modified versions by Sakamoto *et al.* (2003). In brief, the T7RNAP "donor" cells were generated by transfecting 293 cells with both T7RNAP and HIV-1's Env expression vectors. The T7RNAP "acceptor" cells were generated by transfecting 293 cells with the T7RNAP reporter (pT7-IRES-Luciferase) along with either CD4 or CD4Δcyt, GFP or GFP-VCA, and the renilla luciferase expression vectors. At 48 h posttransfection, these cells were cocultivated for 24 h and lysed in the passive lysis buffer to carry out the dual luciferase assay (Promega).

Detection of Fluorescent Signals

The transfected 293 cells were fixed by 4% formaldehyde in PBS at 48 h posttransfection and imaged by using confocal microscopy META 510 (Carl Zeiss, Jene, Germany). For the images showing pseudopodial extensions, images of different focal planes were projected to generate a single image. The transfected H9 cells were imaged similarly at 48 h posttransfection without fixation. The light transmission image was merged with the green fluorescent signal. Alternatively, the transfected cells were analyzed by the flow cytometry (FACS calibur, Becton Dickinson, San Jose, CA).

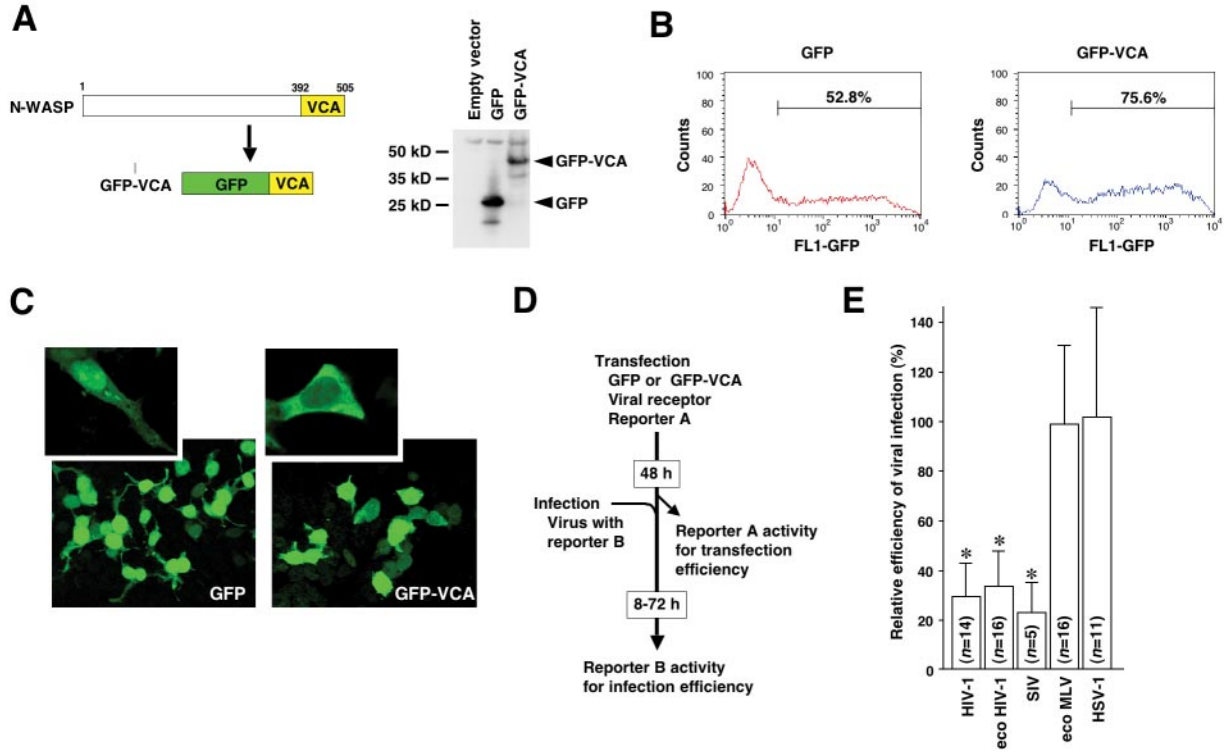

Figure 1. Inhibiting the Arp2/3 complex limited the entry of primate lentiviruses. (A) The carboxy-terminus of N-WASP, VCA domain, was fused to GFP to give rise GFP-VCA. Western blot analysis detected the 41-kDa band, the predicted mol wt for GFP-VCA. (B) The green fluorescence profiles of 293 cells transfected with either GFP or GFP-VCA expression vector were similar to each other as measured by the flow cytometric analysis. (C) GFP-VCA preferentially distributed evenly throughout the cytoplasm. The pseudopodial extension was less active when GFP-VCA was expressed in 293 cells compared with GFP (magnification, ×200; inset, ×400). (D) The experimental procedure was drawn schematically. (E) The relative infection efficiencies of HIV-1, HIV-1 pseudotyped with ecotropic MLV envelope (eco HIV-1), and SIV into cells expressing GFP-VCA were significantly decreased, whereas those of ecotropic MLV (eco MLV) and HSV-1 were not (asterisk, $p < 0.01$). The data represent the average and SD of indicated number of independent experiments.

Western Blot Analysis

Cells were washed with PBS and lysed in a buffer containing 4% SDS, 100 mM Tris-HCl (pH 6.8), 12% 2-ME, 20% glycerol, and bromophenol blue. Samples were boiled for 10 min. Protein lysates approximately equivalent to 5×10^4 cells were separated in SDS-PAGE (Perfect NT Gel, DRC, Tokyo, Japan), transferred to a polyvinylidene fluoride (PVDF) membrane (Immobilon-P^{SQ}, Millipore, Bedford, MA), and blocked with 5% dried nonfat milk (Yuki-Jirushi, Tokyo, Japan) in PBS. For the primary antibody, we used anti-Arp2 antibody H-84 (Santa Cruz Biotechnology, Santa Cruz, CA), antiactin antibody MAB1501 (Chemicon, Temecula, CA), or either an mAb or a polyclonal rabbit antiserum against GFP (Clontech). For the secondary antibody, either a biotinylated anti-mouse antibody (Amersham Pharmacia Biotech, Piscataway, NJ) or a biotinylated anti-rabbit antibody was used. For the tertiary probe, a horseradish peroxidase (HRP)-conjugated streptoavidin (Amersham Pharmacia Biotech) was used. Signals were developed by incubating blots with the chemilumenescent HRP substrate (Amersham Pharmacia Biotech) and detected by using Lumi-Imager F1 (Boehringer Mannheim, Mannheim, Germany).

Reporter Assays

Cells were lysed in the Passive Lysis Buffer (Promega) and the dual luciferase assay was performed to measure both firefly and renilla luciferase activities according to the manufacturer's protocol (Promega). The beta-galactosidase activity was measured by using the LumiGal assay kit according to the manufacturer's protocol (Clontech). The chemiluminescence was detected by Lmax (Nihon Molecular Devices, Tokyo, Japan).

ELISA

The amount of p24 antigen of HIV-1 in the culture supernatants was quantified by using Retro TEK p24 antigen ELISA kit according to the manufacturer's protocol (Zepto Metrix, Buffalo, NY). The signals were measured by Vmax ELISA reader (Nihon Molecular Devices).

Statistical Analysis

The significance of differences was tested by one-way analysis of variance (ANOVA) and Student's t test. P values < 0.05 were considered to be significant.

RESULTS

GFP-VCA Inhibits Infection of Primate Lentiviruses

We first tested whether the viral infection was affected by expressing a potential inhibitor of the Arp2/3 complex GFP-VCA, the VCA domain of N-WASP fused to GFP (Figure 1A). The expression of GFP-VCA protein was verified by Western blot analysis (Figure 1A). The expression levels of GFP-VCA were similar to those of GFP as measured by the flow cytometric analysis at 48 h posttransfection (Figure 1B). GFP-VCA preferentially distributed to the cytoplasm and inhibited the pseudopodial extension compared with GFP alone in agreement with the previous report (Rozelle *et al.*, 2000; Figure 1C). To exclude the possibility that GFP fusion proteins negatively affects the cell surface expression of membrane proteins, we confirmed that the distribution and the levels of transiently and constitutively expressed CD4 and CXCR4 on the cell surface were similar in both GFP- and GFP-VCA–expressing cells as assessed by both confocal microscopy and the flow cytometric analysis (unpublished data).

To evaluate the contribution of the Arp2/3 complex on the viral infection, we used a transient transfection/infection

Table 1. Viruses tested in the receptor-dependent infection system

Virus	Virally encoded reporter	Reporter to normalize infection efficiency	Replication-competency	Infected cells harvested (h postinfection)	Receptor used in this study	S/N ratio[a]
HIV-1	Renilla luciferase	Firefly luciferase	Incompetent	48–72	CD4	4.5
eco HIV-1	Renilla luciferase	Firefly luciferase	Incompetent	48–72	F10	41.2
SIV	Firefly luciferase	Renilla luciferase	Competent	48	CD4 and CCR5	26.4
eco MLV	β-galactosidase	Firefly luciferase	Incompetent	48–72	F10	20.8
HSV-1	β-galactosidase	Firefly luciferase	Competent	8	HigR	207.4

See Figure 1.

[a] The signal-to-noise ratio was calculated by dividing the virally encoded reporter gene activities in the GFP-expressing cells by the background signal. Data from all the trials shown in Figures 1 and 4 were averaged.

system in which target cells were transfected with a mixture of plasmid DNA expressing 1) an Arp2/3 complex inhibitor GFP-VCA, 2) a viral receptor, and 3) a reporter gene to normalize transfection efficiencies (depicted in Figure 1D). Because of the nature of cotransfection, the majority of cells uptook the expression vector for GFP-VCA were transfected with the other plasmids because the mixture of DNA contained fivefold excess amount of the GFP-VCA expressing plasmid. At 48 h posttransfection, a portion of transfected cells were collected to measure the transfection efficiencies and others were challenged by a virus expressing a reporter gene to monitor the efficiency of infection. Various times after infection, cells were lysed and the virally encoded reporter gene activities were measured, which was divided by the transfection efficiencies to normalize. Infection of viruses was restricted to the transfected cells by using viral receptors: human CD4 for HIV-1, human CD4 and CCR5 for SIV, F10 for ecotropic MLV envelope-pseudotyped HIV-1 (eco HIV-1) and ecotropic MLV (eco MLV), human nectin-1 alpha (HigR) for HSV-1. Viruses, receptors, and the combination of reporter genes for each virus were summarized in Table 1. Primarily we targeted HEK293 cells because actin cytoskeletal system is shared among eukaryotes. To monitor HSV-1 infection, CHO-K1 cells were used that lack entry molecules for HSV-1. To monitor the efficiencies of single-round viral infection, we used replication-incompetent HIV-1 and MLV. Alternatively, cells infected with replication-competent viruses were lysed at time points before viruses entered the second replication cycle, except SIV, which required 48 h to give sufficient signal to be detected. Importantly, all the viruses tested in this study were reported to utilize actin cytoskeleton to infect cells as examined by using chemical inhibitors against actin such as cytochalasin (CC; Rosenthal *et al.*, 1985; Kizhatil and Albritton, 1997; Bukrinskaya *et al.*, 1998; Iyengar *et al.*, 1998; Li *et al.*, 1998). The infection efficiencies of viruses into cells expressing GFP were set at 100% throughout the study unless stated and the infection efficiencies into GFP-VCA–expressing cells relative to GFP-expressing cells were calculated. For example, when eco HIV-1 was tested, the firefly luciferase activities representing the transfection efficiencies for GFP- and GFP-VCA–transfected cells were 2,065 and 1,854 relative light unit (RLU), respectively, where the background signal was 3 RLU. The renilla luciferease activities reflecting the infection efficiencies into GFP- and GFP-VCA–transfected cells were 4,018 and 1,254 RLU, respectively, where the background was 15 RLU. In this case, the relative infection efficiency of eco HIV-1 into GFP-VCA expressing cells was 34.4%. The relative infection efficiency was introduced because we were able to integrate data from independent experiments. Results from the indicated number of independent experiments were summarized in Figure 1E. Expression of the GFP-VCA significantly reduced the relative infection efficiencies of HIV-1, eco HIV-1, and SIV (30.3, 35.8, and 22.7%, respectively; $p < 0.01$; Figure 1E), whereas those of eco MLV and HSV-1 (98.5 and 103.5%, respectively; Figure 1E) did not. A 10-fold higher or lower titer of HSV-1 did not affect the results (unpublished data). Consistent with this, the average signal-to-noise ratio did not correlate with the efficiency of inhibition (Figure 1E and Table 1). The GFP-VCA did not inhibit eco MLV but did inhibit the infection of eco HIV-1, suggesting that GFP-VCA's ability to inhibit the infection of eco HIV-1 was eco *env*-independent. It also suggested that the cell surface expression of the F10 was not affected by GFP-VCA expression. In addition, our SIV clone did not encode *nef* and HIV-1 *vpr*, demonstrating that both *nef* and *vpr* were not necessary for primate lentiviruses (HIV-1 and SIV) to infect GFP-VCA–expressing cells efficiently. These results suggested that inhibiting the Arp2/3 complex by GFP-VCA negatively affected the infection of primate lentiviruses.

HIV-1 Pseudotyped with VSV-G Overcomes the Block of Infection by GFP-VCA

To gain insight of the mechanism of GFP-VCA's action to limit primate lentiviral infection, we tested whether the GFP-VCA blocked infection of VSV-G–pseudotyped HIV-1 (VSV-G HIV-1). HIV-1 enters cells by inducing the virus-cell membrane fusion at the cell surface. When HIV-1 was pseudotyped with VSV-G, the route of viral entry became endocytosis (Stein *et al.*, 1987; Maddon *et al.*, 1988). We transfected 293 cells with GFP- or GFP-VCA–expressing plasmid along with one-tenth amount of CD4- and F10-expressing plasmids. Then we enriched transfected cells by using magnetic beads directing toward CD4 at 36–42 h posttransfection. This allowed us to measure the infection efficiencies into the transfected cells only (depicted in Figure 2A). More than 90% of the magnetically selected cells were green fluorescence-positive as examined by the flow cytometric analysis (unpublished data). At 48 h posttransfection, cells were infected either with HIV-1, eco HIV-1 or VSV-G HIV-1. For a comparison, amphotropic MLV (ampho MLV) and VSV-G pseudotyped MLV (VSV-G MLV) were tested in parallel. Infected cells were lysed at 2–3 d postinfection, and the virally encoded reporter gene activities were measured to estimate the relative infection efficiencies (depicted in Figure 2A). For example, when eco HIV-1 was tested in parallel with VSV-G HIV-1, the renilla luciferease activities representing the infection efficiencies of eco HIV-1 into mag-

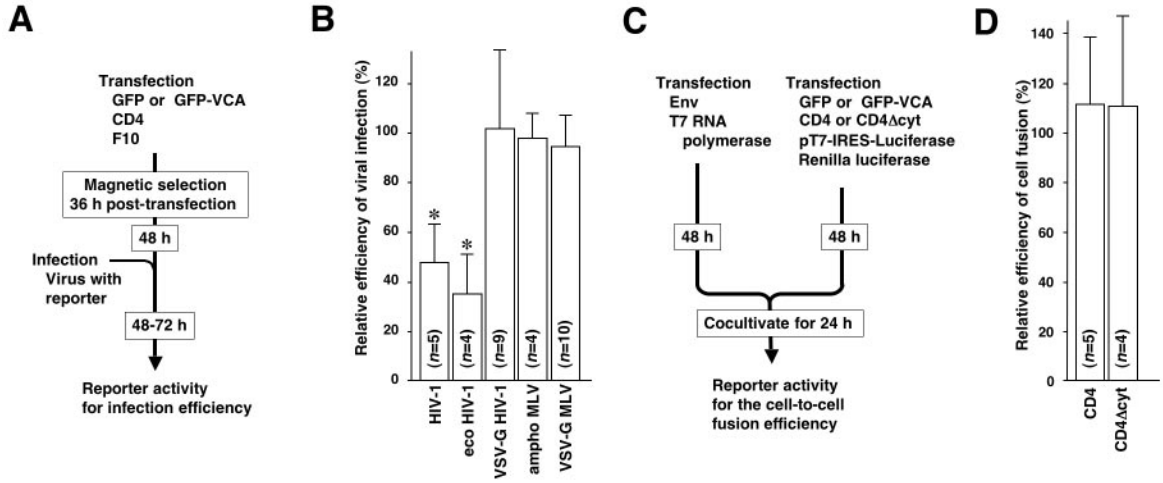

Figure 2. GFP-VCA does not inhibit the infection efficiency of HIV-1 pseudotyped with VSV-G or the membrane fusion induced by the HIV-1's *Env*-CD4 interaction. (A) The experimental procedure using the magnetic selection was drawn schematically. (B) The relative infection efficiencies of HIV-1 and HIV-1 pseudotyped with ecotropic MLV envelope (eco HIV-1) were significantly decreased (asterisk, $p < 0.01$). In contrast, the VSV-G–pseudotyped HIV-1 (VSV-G HIV-1) entered GFP-VCA–expressing cells as efficient as GFP-expressing cells similar to amphotropic MLV (amhpo MLV) and VSV-G–pseudotyped MLV (VSV-G MLV). (C) The experimental procedure for the cell-to-cell fusion assay was drawn schematically. (D) GFP-VCA did not negatively affect the cell-to-cell fusion mediated by HIV-1's *Env* and either the full-length CD4 or the CD4 without the cytoplasmic tail (CD4Δcyt) compared with GFP. The data represent the average and SD of indicated number of independent experiments.

netically selected GFP- and GFP-VCA–expressing cells were 41,968 and 10,117 RLU, respectively, where the background was 30 RLU. In contrast, the renilla luciferase activities of VSV-G HIV-1–infected cells were 6346 RLU for GFP-expressing cells and 5436 RLU for GFP-VCA–expressing cells where the background signal was 30 RLU. In these cases, the relative infection efficiencies of eco and VSV-G HIV-1 into GFP-VCA–expressing cells were 24.1 and 85.6%, respectively. Results from a number of independent experiments are summarized in Figure 2B. The relative infection efficiencies for HIV-1 and eco HIV-1 were significantly reduced when target cells expressed GFP-VCA compared with GFP alone (47.3 and 36.0%, $p < 0.01$, respectively; Figure 2B). The magnitude of inhibition of HIV-1 infection in this assay was smaller than that of the first experimental setup (Figure 1D), presumably because the levels of CD4 on the cell surface might have decreased after the magnetic selection (Figure 1E). On the other hand, the relative infection efficiency for eco HIV-1 (36.0%, $p < 0.01$; Figure 2B) was similar to the first experimental setup, indicating that the magnetic selection did not detectably influence the cellular susceptibility to viral infection. Interestingly, VSV-G HIV-1–infected GFP-VCA–positive cells at efficiencies almost equal to GFP-positive cells (101.7%, Figure 2B). Similarly, both ampho MLV- and VSV-G MLV–infected GFP-VCA–expressing cells as efficient as they did GFP-expressing cells (96.9% for ampho MLV, 93.2% for VSV-G MLV; Figure 2B). In this experimental setup, the signal-to-noise ratio of HIV-1 and eco HIV-1 increased compared with the first experimental system; however, the results remained the same (Figures 1E and 2B, and Table 2). These data indicated that the GFP-VCA was unable to block HIV-1 infection when HIV-1 entered cells through the VSV-G–mediated endocytosis. In other words, the reverse transcription, nuclear import, and integration of HIV-1 genome into the host chromosome were able to proceed in the presence of GFP-VCA.

The Efficiency of the Membrane Fusion Is Not Negatively Affected by GFP-VCA

The membrane fusion is the critical event when enveloped viruses infect cells. We next asked if the expression of GFP-

Table 2. Viruses tested in the magnetic selection system

Virus	Virally encoded reporter	Reporter to normalize infection efficiency	Replication-competency	Receptor used in this study	S/N ratio[a]
HIV-1	Renilla luciferase	Firefly luciferase	Incompetent	CD4	7.2
eco HIV-1	Renilla luciferase	Firefly luciferase	Incompetent	F10	101.3
VSV-G HIV-1	Renilla luciferase	Firefly luciferase	Incompetent		251.6
ampho MLV	β-galactosidase	Firefly luciferase	Incompetent		12.0
VSV-G MLV	β-galactosidase	Firefly luciferase	Incompetent		590.4

See Figure 2.

[a] The signal-to-noise ratio was calculated by dividing the virally encoded reporter gene activities in the GFP-expressing cells by the background signal. Data from all the trials shown in Figure 2 were averaged.

Table 3. Viruses tested in the T7 RNA polymerase system

Virus	Reporter to normalize infection efficiency	Replication-competency	Infected cells harvested (h postinfection)	S/N ratio[a]
IMV	Renillaluciferase	Competent	3	1808.4
Adenovirus	Renillaluciferase	Competent	24	901.3

See Figure 3.

[a] The signal-to-noise ratio was calculated by dividing the luciferase activities in the GFP-expressing cells by the background signal. Data from all the trials shown in Figures 3 and 4 were averaged.

VCA inhibited the membrane fusion through HIV-1's *Env*-receptor interaction. We carried out the cell-to-cell fusion assay in which *Env*-positive cells expressing T7 RNA polymerase (T7RNAP) were fused to the CD4-positive cells carrying the T7RNAP promoter-driven firefly luciferase reporter plasmid (depicted in Figure 2C). The efficiency of the cell-to-cell fusion was measured by the firefly luciferase activity divided by the renilla luciferase activity representing the transfection efficiency. The ratio of the firefly luciferase to renilla luciferase activities in GFP-expressing cells was set at 100%, and the relative efficiencies of cell-to-cell fusion of GFP-VCA–expressing cells were calculated. It revealed that the efficiencies of cell-to-cell fusion initiated by the interaction between HIV-1's *Env* and CD4 were not inhibited when GFP-VCA was expressed in CD4-expressing cells compared with GFP (114%, Figure 2D).

To eliminate a possibility that the GFP-VCA inhibited the expression/distribution of CD4 on the cell surface, we examined whether the CD4 lacking the cytoplasmic domain (CD4Δcyt) was able to support the membrane fusion in the presence of GFP-VCA. Because GFP-VCA distributed throughout the cytoplasm, it was unlikely that the motility of CD4Δcyt on the cell surface was restricted by GFP-VCA. It was found that CD4Δcyt induced the cell-to-cell fusion in the presence of GFP-VCA at efficiencies almost equal to the full length CD4 (113%, Figure 2D). In support of this, enveloped viruses (HSV-1, MLV, and VSV-G HIV-1) were able to infect GFP-VCA–positive cells as efficient as GFP-positive cells (Figures 1E and 2B). In particular, when HSV-1 and ampho MLV enter cells, like HIV-1, the membrane fusion takes place at the cell surface (Fuller and Spear, 1987; McClure *et al.*, 1990; Wittels and Spear, 1991; Nussbaum *et al.*, 1993). These data indicated that the virus-cell membrane fusion was not inhibited by GFP-VCA. According to the data presented hereby, it seemed likely that GFP-VCA did not negatively affect the expression of receptors or viral attachment to receptors, or the virus-cell membrane fusion. Because VSV-G HIV-1–infected cells in the presence of GFP-VCA, we assume that GFP-VCA inhibits HIV-1's life cycle after the membrane fusion before or at the reverse transcription, especially when HIV-1 enters cells through the membrane fusion at cell surface where the viral core is placed in the cortical compartment.

GFP-VCA Inhibits Infection of Intracellular Mature Vaccinia Virus but Not Adenovirus

To test whether the inhibition of viral entry by GFP-VCA was limited to the primate lentiviruses, we examined both intracellular mature vaccinia virus (IMV) and adenovirus. IMV enters cells via the membrane fusion at cell surface, which is accompanied by a drastic actin cytoskeletal reorganization (reviewed by Smith *et al.*, 2002). Adenovirus infects cells through clathrin-dependent endocytosis (Wang *et al.*, 1998). Adenovirus was the only envelope-free virus studied in this article. These viruses encoded T7 RNA polymerase as a reporter (Table 3). To detect the infection signal from transfected/infected cells, we introduced the T7 promoter-driven luciferase reporter into 293 cells (Figure 3A). For example, when IMV was tested, the renilla luciferase activities representing the transfection efficiencies for GFP- and GFP-VCA–transfected cells were 485 and 556 RLU, respectively, where the background signal was 8 RLU. The firefly luciferease activities reflecting the infection efficiencies of virus into GFP- and GFP-VCA–transfected cells were 29,020 and 10,044 RLU, respectively, where the background was 23 RLU. In this case, the relative infection efficiency of IMV into GFP-VCA–expressing cells was 30.3%. Results from a number of independent experiments were summarized in Figure 3B. The relative infection efficiency of IMV was significantly reduced (30.6%, $p < 0.01$; Figure 3B), whereas adenovirus-infected GFP-VCA–expressing cells as efficiently as GFP-expressing cells (98.3%, Figure 3B). IMV gave the highest signal-to-noise ratio throughout the study, yet its infection was blocked efficiently by GFP-VCA (Table 3). Considering all the signal-to-noise data, it was suggested that the signal-to-noise ratio did not positively correlate with the magnitude of inhibition of viral infection. Ten-fold higher or lower titer of either IMV or adenovirus did not affect the results

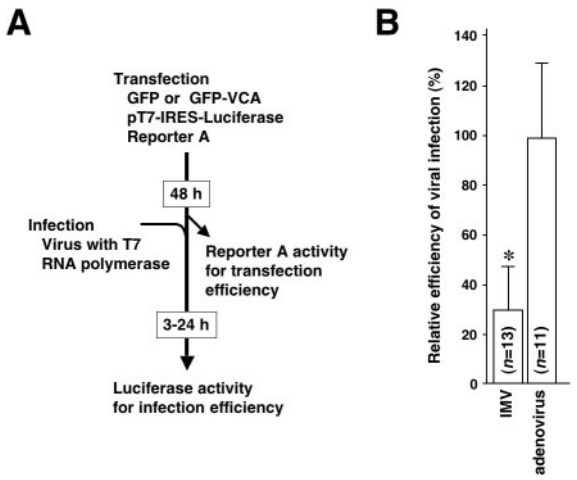

Figure 3. Limiting infection of IMV but not adenovirus by inhibiting the Arp2/3 complex. (A) The experimental procedure was drawn schematically. (B) The significant decrease of relative infection efficiency of IMV, but not adenovirus, was observed (asterisk, $p < 0.01$). The data represent the average and SD of indicated number of independent experiments.

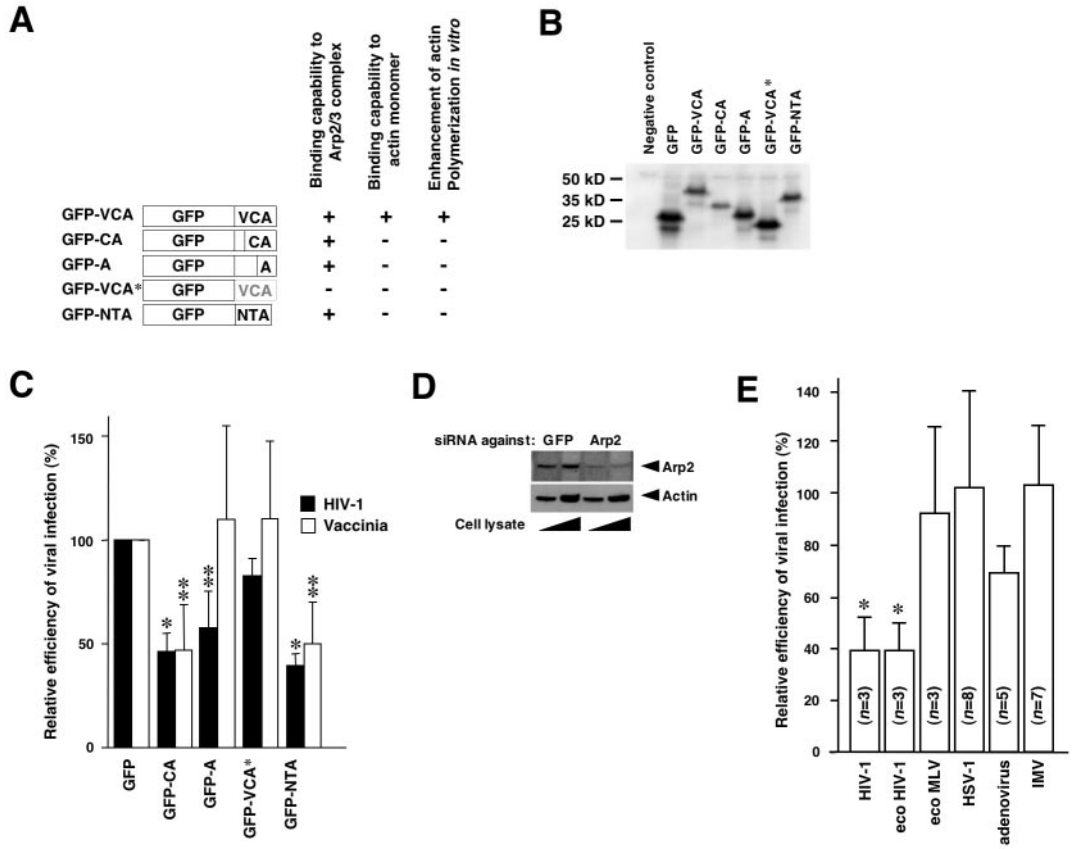

Figure 4. Inhibitory effects of GFP-VCA derivatives, GFP-NTA, and siRNA against Arp2 on the infection of both HIV-1 and IMV. (A) Schematic drawing of GFP-VCA derivatives and GFP-NTA. (B) Western blot analysis detected 30-, 41-, 32-, 30-, 28-, and 37-kDa bands, each predicted mol wt for GFP, GFP-VCA, -CA, -A, VCA*, and -NTA, respectively. (C) The relative infection efficiencies of HIV-1 (■) and IMV (□) were significantly inhibited when cells expressed GFP-CA and GFP-NTA (asterisk, $p < 0.01$; double asterisks, $p < 0.05$). Expression of GFP-A significantly reduced the relative infection efficiency for HIV-1 but not for IMV. GFP-VCA* did not detectably inhibited infection of both viruses. The data represent the average and SD of more than three independent experiments. (D) The siRNA directed against Arp2 down-modulated expression of Arp2 by 73.5% on the average, whereas the expression of siRNA against GFP did not as demonstrated by Western blot analysis in which 293 cell lysates corresponding to the 5×10^4 or 2×10^5 were analyzed at 2 d posttransfection. (E) Introducing siRNA against Arp2 significantly reduced the relative infection efficiencies of HIV-1 and HIV-1 pseudotyped with ecotropic MLV envelope (eco HIV-1; asterisk, $p < 0.01$) but not ecotropic MLV (eco MLV), HSV-1, adenovirus, and IMV. The data represent the average and SD of indicated number of independent experiments.

(unpublished data). These data suggested that inhibiting the Arp2/3 complex by GFP-VCA negatively affected infection of IMV as well as primate lentiviruses. We focused on HIV-1 and IMV for the further studies.

GFP-VCA's Ability to Nucleate Actin Filament Is Not Necessary to Inhibit Viral Entry

We attempted to locate the domain within VCA responsible for the inhibition of HIV-1 and IMV infection. We generated a series of truncated GFP-VCA mutants (Figure 4A). Their functions were also summarized according to the previous reports (Figure 4A; Takenawa and Miki, 2001; Weaver *et al.*, 2003). Expression of each mutant was verified in Western blot analysis (Figure 4B). Introducing a stop codon into GFP-VCA after the GFP open reading frame allowed VCA-encoding RNA to be expressed but not VCA protein (GFP-VCA*). Expression of GFP-VCA* did not inhibit infection of both HIV-1 and IMV (82.9 and 112.6%, respectively; Figure 4C), suggesting that the inhibition of viral entry attributed to the VCA protein, not the VCA-encoding RNA (Figure 4C). GFP-CA retained the ability to limit both HIV-1 and IMV infection (46.7 and 46.4%, $p < 0.01$ and $p < 0.05$, respectively, Figure 4C). Expression of GFP-A inhibited HIV-1 infection less efficiently than other derivatives (57.7%, $p < 0.05$; Figure 4C). However, GFP-A was unable to limit IMV infection (110.8%, Figure 4C) although synthetic peptides of A subdomain has been shown to retain the binding affinity to the Arp2/3 complex as high as VCA in vitro (Panchal *et al.*, 2003). These data suggested that the V subdomain was not required for the inhibition of HIV-1 and IMV infection. It seemed likely that C and A subdomains functioned cooperatively in vivo to inhibit infection of both HIV-1 and IMV.

To further verify that the reduction of viral infection efficiencies was due to the inhibition of Arp2/3 complex functions, we have tested whether another potential Arp2/3 complex inhibitor NTA, amino-terminal acidic domain of cortactin (amino acids 1–84), was also able to limit both HIV-1 and IMV infection as did VCA. Cortactin is unrelated to WASP family of proteins but is able to bind the Arp2/3 complex through the NTA domain. Expression of GFP-NTA was verified by Western blot analysis (Figure 4B). As expected, GFP-NTA reduced the infection efficiencies of both

HIV-1 and IMV (39 and 50%, $p < 0.01$ and $p < 0.05$, respectively; Figure 4C). These data confirmed that inhibiting functions of the Arp2/3 complex was indeed responsible for limiting both HIV-1 and IMV infection. As GFP-NTA lacked the ability to nucleate actin filaments similar to GFP-CA and because of the reported functions of CA subdomains (Figure 4A), it was strongly suggested that, not their abilities to enhance actin nucleation, but GFP fusion proteins' abilities to bind the Arp2/3 complex was primarily important to inhibit viral infection.

In addition, we tested whether down-regulating expression of Arp2 by using siRNA technique inhibited both HIV-1 and IMV infection. The GFP-VCA and -NTA were able to inhibit functions of Arp2/3 complex by binding to it directly, whereas siRNA against Arp2 down-modulated expression of Arp2, therefore decreasing the number of Arp2/3 complex. Because siRNA against Arp2 was not able to inhibit the function of preexisting Arp2/3 complex directly, it was expected that siRNA against Arp2 should be able to limit viral infection, if any, less efficiently than GFP-VCA. Transfecting the plasmid vector expressing siRNA directing against Arp2 reduced the expression of endogenously expressed Arp2–26.5% in 293 cells as demonstrated by Western blotting analysis (Figure 4D). Viral infection efficiencies were measured using the experimental setups (Figures 1D and 3A) except the GFP or GFP-VCA expression plasmid was replaced with the siRNA expression vectors against GFP or Arp2. When siRNA directing toward GFP was set as 100%, the relative efficiencies of both HIV-1 and eco HIV-1 infection in cells expressing siRNA against Arp2 became 39.4 and 39.1%, respectively (both, $p < 0.01$; Figure 4E). Adenovirus infection was slightly inhibited by the siRNA against Arp2 (69.4%, Figure 4E). However, the relative infection efficiencies of eco MLV, HSV-1, and IMV were not significantly reduced by siRNA directed toward Arp2 (91.3, 103.8, and 104.4%, respectively, Figure 4E). Given that the other two Arp2/3 inhibitors were able to limit IMV and HIV-1 infection, it seemed reasonable to speculate that the inhibition of HIV-1 infection by siRNA was due to the down-modulation of newly synthesized Arp2. However, we were unable to limit the infection of IMV by siRNA against Arp2. We assumed that this was either because siRNA was unable to down-regulate expression of Arp2, therefore Arp2/3 complex, at levels sufficient to block the entry of IMV or the number of the preexisting Arp2/3 complex might be sufficient to support IMV infection, or both.

HIV-1 Replication Is Negatively Affected When GFP-VCA Is Constitutively Expressed in H9 Cells

Finally, we asked whether the replication of HIV-1 was inhibited in T-cells, one of the natural targets of HIV-1. To do this, we isolated H9 cell clones either expressing GFP or GFP-VCA constitutively by infecting H9 cells with MLV vector followed by the limiting dilution. Introducing expression plasmid for GFP-VCA did not alter the morphology of H9 cells compared with GFP-expressing cells or untransfected cells when observed under the confocal microscopy at 48 h posttransfection (Figure 5A) as well as stable cell clones (unpublished data). H9 GFP-VCA clones proliferated at speed indistinguishable from H9 GFP clones (unpublished data). We verified the expression of GFP and GFP-VCA in isolated clones by Western blot analysis (Figure 5B). However, the average expression levels of GFP-VCA appeared low compared with those of GFP in H9 clones (Figure 5B). We infected six H9-GFP and three H9-GFP-VCA clones with a replication-competent HIV-1 (HXB2) and collected culture supernatants at different time points to monitor the viral

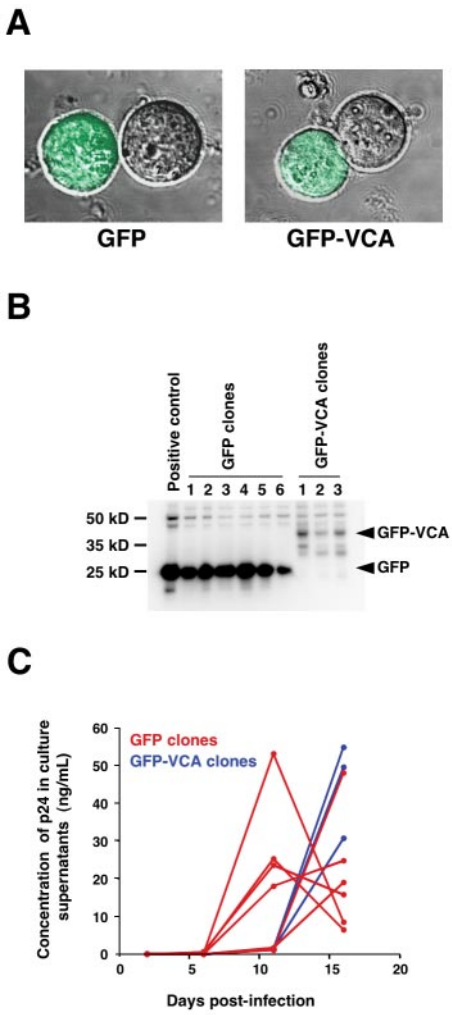

Figure 5. Slow replication kinetics of HIV-1 in H9 cells expressing GFP-VCA constitutively. (A) The morphology of H9 cells was not drastically altered when GFP-VCA was expressed compared with GFP or untransfected cells. The green fluorescent image was merged with the transmission image (magnification, ×630). (B) H9 clones stably expressed GFP or GFP-VCA as demonstrated by Western blot analysis (arrowheads). (C) The amount of p24 antigen in the culture supernatants accumulated rapidly in H9-GFP cell clones (red), whereas H9-GFP-VCA clones did not support the efficient HIV-1 replication (blue). Similar results were obtained by two independent experiments.

replication by measuring the amount of p24 viral antigen. The replication kinetics of HIV-1 in GFP-expressing H9 clones showed a rapid propagation of HIV-1 in culture. In contrast, the amount of p24 in the culture supernatants of H9 GFP-VCA clones did not accumulate, suggesting that the HIV-1 replication was substantially suppressed in H9 GFP-VCA clones (Figure 5C). The replication assay was carried out twice consecutively and similar data were obtained. On the average, the peak of HIV-1 replication kinetics in GFP-VCA clones delayed a week compared with GFP clones. The maximum amount of p24 in the culture supernatants of H9 GFP-VCA clones did not appear different from those of H9 GFP clones.

We next examined whether the viruses propagated in H9 GFP-VCA clones were mutants capable of replicating in the presence of GFP-VCA. We isolated viral RNA from the

culture supernatants of a H9 GFP clone and three H9 GFP-VCA clones and sequenced the *gag/pro/pol* region because the GFP-VCA's ability to limit HIV-1 infection did not depend on *Env*, *Nef*, *Vpr*, and *Rev*. However, we could not find any nucleic acid alterations when the viral sequences from an H9 GFP-VCA culture were compared with the one from an H9 GFP culture. These data suggested that the levels of GFP-VCA in H9 clones might be insufficient to confer the selective advantage for mutant viruses to take over the wild-type HIV-1. We found that the late phase of HIV-1 viral life cycle was slightly affected by GFP-VCA. Transfecting proviral DNA into 293 T-cells along with the expression vector for GFP-VCA yielded fewer amount of p24 antigen in the culture supernatant (72%) compared with GFP alone. Taken together, the decreased replication kinetics of HIV-1 in H9 GFP-VCA was assumed to be mostly due to the inhibition of the early phase, partly the late phase, of HIV-1's life cycle. These data demonstrated that the constitutive inhibition of the Arp2/3 complex by expressing GFP-VCA limited efficient replication of HIV-1 in T-cells as well as epithelial cell systems.

DISCUSSION

We have demonstrated that the Arp2/3 complex contributes to the efficient infection of both primate lentiviruses (HIV-1 and SIV) and IMV but not MLV, HSV-1, and adenovirus. Actin cytoskeleton has been shown to play a role in the infection of all the viruses tested in this study according to previous studies using the chemical actin inhibitor (Rosenthal *et al.*, 1985; Kizhatil and Albritton, 1997; Bukrinskaya *et al.*, 1998; Iyengar *et al.*, 1998; Li *et al.*, 1998; Locker *et al.*, 2000). In addition, the Arp2/3 complex-mediated actin nucleation is sensitive to CC (Welch *et al.*, 1998). Therefore, GFP-VCA's ability to limit infection of primate lentiviruses and IMV might be a part of, if not all, the mechanism by which CC reduced the efficiency of viral infection. In other words, primate lentiviruses and IMV might utilize the Arp2/3 complex-dependent actin polymerization system to support their early phase of viral life cycles. In contrast, MLV, HSV-1, and adenovirus might utilize actin to enter cells in an Arp2/3 complex-independent manner. Perhaps, other functional aspects of actin are important for their efficient infection such as the actin cable-dependent trafficking system. Our data clearly demonstrated that the different viruses use actin system differently. It was reported that the infection of HIV-1 was inhibited by CC at least two different levels: 1) by limiting viral receptor/coreceptor clustering upon viral attachment (Iyengar *et al.*, 1998); and 2) by disrupting establishment of active reverse transcription complex (Bukrinskaya *et al.*, 1998). Our findings suggest a possible involvement of the Arp2/3 complex in the latter process or a presence of another actin polymerization-dependent step between two processes.

What is the molecular mechanism by which the Arp2/3 complex supports infection of both primate lentiviruses and IMV? One of the possibilities is that these viruses may activate the Arp2/3 complex and nucleate actin filaments to support their entry. It has been reported that an acidic motif DDW or DEW can be found among cellular Arp2/3 complex-binding proteins including WASP, cortactin, and MyoD as well as *Listeria monocytogenes* surface protein ActA (Weed and Parsons, 2001). We are unable to find such a binding motif in proteins encoded by both HIV-1 and SIV. Therefore, these viruses may not activate Arp2/3 complex due to a direct interaction between viral gene products and Arp2/3 complex. There are two regulatory pathways known to activate the Arp2/3 complex. One is WASP/WAVE pathway and the other being cortactin pathway. Expression of the dominant-negative derivatives of N-WASP, WAVEs, and cortactin were unable to limit the infection of both HIV-1 and IMV (unpublished observation, consistent with the Locker's finding, Locker *et al.*, 2000). The dominant-negative derivative of cdc42, RhoGTPase family protein that locates upstream of WASP/WAVE pathway, was also unable to reduce the relative infection efficiencies of both viruses (unpublished observation). These data implied that the activation of Arp2/3 complex upon infection of both lentiviruses and IMV might be mediated by novel virus-host interactions. Inhibiting the Arp2/3 complex by GFP-VCA did not drastically reduce the efficiency of HIV-1 production as did that of HIV-1 infection, suggesting that the incoming HIV-1 might have something unique which budding virus lacks. We speculate that viral gene products cleaved by HIV-1's protease may be responsible to induce activation of Arp2/3 complex because viral protease become active when viral particles are released from cells such that the cleaved proteins are present at high concentrations only in mature virus particles. VV encodes envelope protein A36R that binds adaptor proteins Nck, Wip, Grb2 that recruits and activates WASP-Arp2/3 complex system (Frischknecht *et al.*, 1999; Rietdorf *et al.*, 2001; Scaplehorn *et al.*, 2002). These molecular interactions are known to be important for vaccinia virus to bud from infected cells as extracellular enveloped virus (EEV). However, IMV does not have A36R on its envelope. Accordingly, IMV should initiate activation of Arp2/3 complex via A36R-independent mechanisms.

On the basis of our data as well as previous observations, we propose models in which the Arp2/3 complex plays a role in the entry of both primate lentiviruses and IMV. HIV-1 enters cells via the membrane fusion on the cell surface (Stein *et al.*, 1987; Maddon *et al.*, 1988). The viral core complex is released to the cytoplasm immediately after the membrane fusion over the cortical layer. Our model is that the viral core components, independent of *Env*, *Nef*, *Vpr*, and *Rev*, recruit adaptor proteins and activate the Arp2/3 complex to generate mechanical force by which HIV-1's core complex passes through the cortical layer and migrates toward the nucleus efficiently (Figure 6A). McDonald *et al.* (2002) had shown that the microtubule system supports long-distance movement of HIV-1's core complex. It is possible that lentiviruses utilize the Arp2/3 complex-mediated active transport system to get access to a subcellular compartment where they meet microtubule system. Consistent with our model, a short-distance rapid movement of HIV-1's core was observed in the time-lapse imaging, which suggested a presence of an actin polymerization-dependent transport (McDonald *et al.*, 2002). On the other hand, IMV enters cells via the membrane fusion at the cell surface as suggested by the intensive studies including electron microscopic studies (reviewed in Smith *et al.*, 2002). IMV infection induces the formation of actin-rich cell surface protrusions partly due to GTPase *Rac1* signaling (Locker *et al.*, 2000) and is inhibited by treating cells with CCD (Vanderplasschen *et al.*, 1998; Locker *et al.*, 2000). Taken together, the Arp2/3 complex-mediated actin polymerization may be required for not only the late phase but also the early phase of IMV's life cycle, specifically at the postmembrane fusion processes (Figure 6B). Also, it is necessary to reorganize the cortical actin network to transport the virus-core toward the cytoplasmic subcompartment where the vaccinia virus replicates. The Arp2/3 complex may play a role in the latter process (Figure 6B). In any case, IMV induces relatively global cytoskeletal reorganization in which a substantial

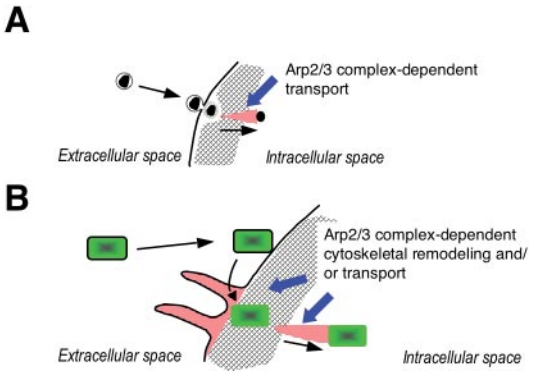

Figure 6. Models in which the Arp2/3 complex supports infection of both primate lentiviruses and IMV. (A) Primate lentiviruses enter cells via membrane fusion at cell surface. After membrane fusion, viral gene products might initiate activation of Arp2/3 complex-dependent actin polymerization (red) behind the viral core to cross the cortical layer (gray). (B) IMV also enters cells via membrane fusion at the cell surface. At or soon after the attachment, the dynamic actin cytoskeletal reorganization takes place that depends partly on the Arp2/3 complex-mediated actin polymerization (red), which may facilitate viral entry. Alternatively, the Arp2/3 complex-mediated actin polymerization (red) powers the viral core (green) to migrate toward the cytoplasmic compartment in which vaccinia virus replicates.

number of Arp2/3 complex should participate. This may account for the less efficient block of IMV's infection by both GFP-A and siRNA directing against Arp2 (Figure 4, C and E).

Our finding suggested a new therapeutic target to control HIV-1 replication in AIDS patients. We should be able to limit HIV-1 replication by inhibiting the HIV-1's ability to activate Arp2/3 complex by a small chemical compound. It is underway to determine which viral gene product is responsible to activate Arp2/3 complex.

ACKNOWLEDGMENTS

We thank Drs. Hironori Sato, Bill Sugden, and Tsutomu Murakami for critical reading of the manuscript and Yuko Futahashi for the technical assistance. We also thank Drs. T. Takenawa, A. Yamashita, J. Young, E. Freed, P. G. Spear, Y. Takai, S. Takase-Yoden, W. Sugiura, and K. Mori for generously sharing reagents and equipments. This work was partly supported by both the Japan Health Science Foundation and a grant from Japanese Ministry of Health, Labor, and Welfare.

REFERENCES

Aoki, Y., Aizaki, H., Shimoike, T., Tani, H., Ishii, K., Saito, I., Matsuura, Y., and Miyamura, T. (1998). A human liver cell line exhibits efficient translation of HCV RNAs produced by a recombinant adenovirus expressing T7 RNA polymerase. Virology *250*, 140–150.

Bukrinskaya, A., Brichacek, B., Mann, A., and Stevenson, M. (1998). Establishment of a functional human immunodeficiency virus type 1 (HIV-1) reverse transcription complex involves the cytoskeleton. J. Exp. Med. *188*, 2113–2125.

Cantarelli, V.V., Takahashi, A., Akeda, Y., Nagayama, K., and Honda, T. (2000). Interaction of enteropathogenic or enterohemorrhagic *Escherichia coli* with HeLa cells results in translocation of cortactin to the bacterial adherence site. Infect. Immun. *68*, 382–386.

Castellano, F., Le Clainche, C., Patin, D., Carlier, M.F., and Chavrier, P. (2001). A WASp-VASP complex regulates actin polymerization at the plasma membrane. EMBO J. *20*, 5603–5614.

Cudmore, S., Reckmann, I., and Way, M. (1997). Viral manipulations of the actin cytoskeleton. Trends Microbiol. *5*, 142–148.

Dean, H.J., Terhune, S.S., Shieh, M.T., Susmarski, N., and Spear, P.G. (1994). Single amino acid substitutions in gD of herpes simplex virus 1 confer resistance to gD-mediated interference and cause cell-type-dependent alterations in infectivity. Virology *199*, 67–80.

Dehio, C., Prevost, M.C., and Sansonetti, P.J. (1995). Invasion of epithelial cells by *Shigella flexneri* induces tyrosine phosphorylation of cortactin by a pp60c-src-mediated signalling pathway. EMBO J. *14*, 2471–2482.

Fawaz, F.S., van Ooij, C., Homola, E., Mutka, S.C., and Engel, J.N. (1997). Infection with *Chlamydia trachomatis* alters the tyrosine phosphorylation and/or localization of several host cell proteins including cortactin. Infect. Immun. *65*, 5301–5308.

Flanagan, L.A., Chou, J., Falet, H., Neujahr, R., Hartwig, J.H., and Stossel, T.P. (2001). Filamin A, the Arp2/3 complex, and the morphology and function of cortical actin filaments in human melanoma cells. J. Cell Biol. *155*, 511–517.

Frischknecht, F., Moreau, V., Rottger, S., Gonfloni, S., Reckmann, I., Superti-Furga, G., and Way, M. (1999). Actin-based motility of vaccinia virus mimics receptor tyrosine kinase signalling. Nature *401*, 926–929.

Fuerst, T.R., Niles, E.G., Studier, F.W., and Moss, B. (1986). Eukaryotic transient-expression system based on recombinant vaccinia virus that synthesizes bacteriophage T7 RNA polymerase. Proc. Natl. Acad. Sci. USA *83*, 8122–8126.

Fuller, A.O., and Spear, P.G. (1987). Anti-glycoprotein D antibodies that permit adsorption but block infection by herpes simplex virus 1 prevent virion-cell fusion at the cell surface. Proc. Natl. Acad. Sci. USA *84*, 5454–5458.

Gournier, H., Goley, E.D., Niederstrasser, H., Trinh, T., and Welch, M.D. (2001). Reconstitution of human Arp2/3 complex reveals critical roles of individual subunits in complex structure and activity. Mol. Cell *8*, 1041–1052.

Gruenheid, S., and Finlay, B.B. (2003). Microbial pathogenesis and cytoskeletal function. Nature *422*, 775–781.

Gundlach, B.R. *et al.* (1997). Construction, replication, and immunogenic properties of a simian immunodeficiency virus expressing interleukin-2. J. Virol. *71*, 2225–2232.

Harlander, R.S., Way, M., Ren, Q., Howe, D., Grieshaber, S.S., and Heinzen, R.A. (2003). Effects of ectopically expressed neuronal Wiskott-Aldrich syndrome protein domains on *Rickettsia rickettsii* actin-based motility. Infect. Immun. *71*, 1551–1556.

Higgs, H.N., Blanchoin, L., and Pollard, T.D. (1999). Influence of the C terminus of Wiskott-Aldrich syndrome protein (WASp) and the Arp2/3 complex on actin polymerization. Biochemistry *38*, 15212–15222.

Higgs, H.N., and Pollard, T.D. (2001). Regulation of actin filament network formation through ARP2/3 complex: activation by a diverse array of proteins. Annu. Rev. Biochem. *70*, 649–676.

Ichihashi, Y., and Oie, M. (1996). Neutralizing epitope on penetration protein of vaccinia virus. Virology *220*, 491–494.

Iyengar, S., Hildreth, J.E., and Schwartz, D.H. (1998). Actin-dependent receptor colocalization required for human immunodeficiency virus entry into host cells. J. Virol. *72*, 5251–5255.

Kizhatil, K., and Albritton, L.M. (1997). Requirements for different components of the host cell cytoskeleton distinguish ecotropic murine leukemia virus entry via endocytosis from entry via surface fusion. J. Virol. *71*, 7145–7156.

Krause, M., Sechi, A.S., Konradt, M., Monner, D., Gertler, F.B., and Wehland, J. (2000). Fyn-binding protein (Fyb)/SLP-76-associated protein (SLAP), Ena/vasodilator-stimulated phosphoprotein (VASP) proteins and the Arp2/3 complex link T cell receptor (TCR) signaling to the actin cytoskeleton. J. Cell Biol. *149*, 181–194.

Li, E., Stupack, D., Bokoch, G.M., and Nemerow, G.R. (1998). Adenovirus endocytosis requires actin cytoskeleton reorganization mediated by Rho family GTPases. J. Virol. *72*, 8806–8812.

Locker, J.K., Kuehn, A., Schleich, S., Rutter, G., Hohenberg, H., Wepf, R., and Griffiths, G. (2000). Entry of the two infectious forms of vaccinia virus at the plasma membrane is signaling-dependent for the IMV but not the EEV. Mol. Biol. Cell *11*, 2497–2511.

Machesky, L.M., and Insall, R.H. (1998). Scar1 and the related Wiskott-Aldrich syndrome protein, WASP, regulate the actin cytoskeleton through the Arp2/3 complex. Curr. Biol. *8*, 1347–1356.

Machesky, L.M., Mullins, R.D., Higgs, H.N., Kaiser, D.A., Blanchoin, L., May, R.C., Hall, M.E., and Pollard, T.D. (1999). Scar, a WASp-related protein, activates nucleation of actin filaments by the Arp2/3 complex. Proc. Natl. Acad. Sci. USA *96*, 3739–3744.

Maddon, P.J., McDougal, J.S., Clapham, P.R., Dalgleish, A.G., Jamal, S., Weiss, R.A., and Axel, R. (1988). HIV infection does not require endocytosis of its receptor, CD4. Cell *54*, 865–874.

Marchand, J.B., Kaiser, D.A., Pollard, T.D., and Higgs, H.N. (2001). Interaction of WASP/Scar proteins with actin and vertebrate Arp2/3 complex. Nat. Cell Biol. *3*, 76–82.

May, R.C., Caron, E., Hall, A., and Machesky, L.M. (2000). Involvement of the Arp2/3 complex in phagocytosis mediated by FcgammaR or CR3. Nat. Cell Biol. *2*, 246–248.

McClure, M.O., Sommerfelt, M.A., Marsh, M., and Weiss, R.A. (1990). The pH independence of mammalian retrovirus infection. J. Gen. Virol. *71*, 767–773.

McDonald, D., Vodicka, M.A., Lucero, G., Svitkina, T.M., Borisy, G.G., Emerman, M., and Hope, T.J. (2002). Visualization of the intracellular behavior of HIV in living cells. J. Cell Biol. *159*, 441–452.

McGee, K., Zettl, M., Way, M., and Fallman, M. (2001). A role for N-WASP in invasin-promoted internalisation. FEBS Lett. *509*, 59–65.

Miki, H., Miura, K., and Takenawa, T. (1996). N-WASP, a novel actin-depolymerizing protein, regulates the cortical cytoskeletal rearrangement in a PIP2-dependent manner downstream of tyrosine kinases. EMBO J. *15*, 5326–5335.

Miki, H., and Takenawa, T. (1998). Direct binding of the verprolin-homology domain in N-WASP to actin is essential for cytoskeletal reorganization. Biochem. Biophys. Res. Commun. *243*, 73–78.

Moreau, V., Frischknecht, F., Reckmann, I., Vincentelli, R., Rabut, G., Stewart, D., and Way, M. (2000). A complex of N-WASP and WIP integrates signalling cascades that lead to actin polymerization. Nat. Cell Biol. *2*, 441–448.

Nussbaum, O., Broder, C.C., and Berger, E.A. (1994). Fusogenic mechanisms of enveloped-virus glycoproteins analyzed by a novel recombinant vaccinia virus-based assay quantitating cell fusion-dependent reporter gene activation. J. Virol. *68*, 5411–5422.

Nussbaum, O., Roop, A., and Anderson, W.F. (1993). Sequences determining the pH dependence of viral entry are distinct from the host range-determining region of the murine ecotropic and amphotropic retrovirus envelope proteins. J. Virol. *67*, 7402–7405.

Panchal, S.C., Kaiser, D.A., Torres, E., Pollard, T.D., and Rosen, M.K. (2003). A conserved amphipathic helix in WASP/Scar proteins is essential for activation of Arp2/3 complex. Nat. Struct. Biol. *10*, 591–598.

Pantaloni, D., Le Clainche, C., and Carlier, M.F. (2001). Mechanism of actin-based motility. Science *292*, 1502–1506.

Ragheb, J.A., and Anderson, W.F. (1994). pH-independent murine leukemia virus ecotropic envelope-mediated cell fusion: implications for the role of the R peptide and p12E TM in viral entry. J. Virol. *68*, 3220–3231.

Rietdorf, J., Ploubidou, A., Reckmann, I., Holmstrom, A., Frischknecht, F., Zettl, M., Zimmermann, T., and Way, M. (2001). Kinesin-dependent movement on microtubules precedes actin-based motility of vaccinia virus. Nat. Cell Biol. *3*, 992–1000.

Robinson, R.C., Turbedsky, K., Kaiser, D.A., Marchand, J.B., Higgs, H.N., Choe, S., and Pollard, T.D. (2001). Crystal structure of Arp2/3 complex. Science *294*, 1679–1684.

Rohatgi, R., Ma, L., Miki, H., Lopez, M., Kirchhausen, T., Takenawa, T., and Kirschner, M.W. (1999). The interaction between N-WASP and the Arp2/3 complex links Cdc42-dependent signals to actin assembly. Cell *97*, 221–231.

Rosenthal, K.S., Perez, R., and Hodnichak, C. (1985). Inhibition of herpes simplex virus type 1 penetration by cytochalasins B and D. J. Gen. Virol. *66*, 1601–1605.

Rozelle, A.L. *et al.* (2000). Phosphatidylinositol 4,5-bisphosphate induces actin-based movement of raft-enriched vesicles through WASP-Arp2/3. Curr. Biol. *10*, 311–320.

Sakamoto, T., Ushijima, H., Okitsu, S., Suzuki, E., Sakai, K., Morikawa, S., and Muller, W.E. (2003). Establishment of an HIV cell-cell fusion assay by using two genetically modified HeLa cell lines and reporter gene. J. Virol. Methods *114*, 159–166.

Sakisaka, T. *et al.* (2001). Requirement of interaction of nectin-1alpha/HveC with afadin for efficient cell-cell spread of herpes simplex virus type 1. J. Virol. *75*, 4734–4743.

Scaplehorn, N., Holmstrom, A., Moreau, V., Frischknecht, F., Reckmann, I., and Way, M. (2002). Grb2 and Nck act cooperatively to promote actin-based motility of vaccinia virus. Curr. Biol. *12*, 740–745.

Smith, G.L., Vanderplasschen, A., and Law, M. (2002). The formation and function of extracellular enveloped vaccina virus. J. Gen. Virol. *83*, 2915–2931.

Stein, B.S., Gowda, S.D., Lifson, J.D., Penhallow, R.C., Bensch, K.G., and Engleman, E.G. (1987). pH-independent HIV entry into CD4-positive T cells via virus envelope fusion to the plasma membrane. Cell *49*, 659–668.

Takase-Yoden, S., and Watanabe, R. (1999). Contribution of virus-receptor interaction to distinct viral proliferation of neuropathogenic and nonneuropathogenic murine leukemia viruses in rat glial cells. J. Virol. *73*, 4461–4464.

Takenawa, T., and Miki, H. (2001). WASP and WAVE family proteins: key molecules for rapid rearrangement of cortical actin filaments and cell movement. J. Cell Sci. *114*, 1801–1809.

Uruno, T., Liu, J., Zhang, P., Fan, Y., Egile, C., Li, R., Mueller, S.C., and Zhan, X. (2001). Activation of Arp2/3 complex-mediated actin polymerization by cortactin. Nat. Cell Biol. *3*, 259–266.

Vanderplasschen, A., Hollinshead, M., and Smith, G.L. (1998). Intracellular and extracellular vaccinia virions enter cells by different mechanisms. J. Gen. Virol. *79*, 877–887.

Wang, K., Huang, S., Kapoor-Munshi, A., and Nemerow, G. (1998). Adenovirus internalization and infection require dynamin. J. Virol. *72*, 3455–3458.

Weaver, A.M., Karginov, A.V., Kinley, A.W., Weed, S.A., Li, Y., Parsons, J.T., and Cooper, J.A. (2001). Cortactin promotes and stabilizes Arp2/3-induced actin filament network formation. Curr. Biol. *11*, 370–374.

Weaver, A.M., Young, M.E., Lee, W.L., and Cooper, J.A. (2003). Integration of signals to the Arp2/3 complex. Curr. Opin. Cell Biol. *15*, 23–30.

Weed, S.A., Karginov, A.V., Schafer, D.A., Weaver, A.M., Kinley, A.W., Cooper, J.A., and Parsons, J.T. (2000). Cortactin localization to sites of actin assembly in lamellipodia requires interactions with F-actin and the Arp2/3 complex. J. Cell Biol. *151*, 29–40.

Weed, S.A., and Parsons, J.T. (2001). Cortactin: coupling membrane dynamics to cortical actin assembly. Oncogene *20*, 6418–6434.

Welch, M.D., Rosenblatt, J., Skoble, J., Portnoy, D.A., and Mitchison, T.J. (1998). Interaction of human Arp2/3 complex and the *Listeria monocytogenes* ActA protein in actin filament nucleation. Science *281*, 105–108.

Wittels, M., and Spear, P.G. (1991). Penetration of cells by herpes simplex virus does not require a low pH-dependent endocytic pathway. Virus Res. *18*, 271–290.

Zalevsky, J., Grigorova, I., and Mullins, R.D. (2001). Activation of the Arp2/3 complex by the *Listeria* acta protein. Acta binds two actin monomers and three subunits of the Arp2/3 complex. J. Biol. Chem. *276*, 3468–3475.

Zhang, J. *et al.* (1999). Antigen receptor-induced activation and cytoskeletal rearrangement are impaired in Wiskott-Aldrich syndrome protein-deficient lymphocytes. J. Exp. Med. *190*, 1329–1342.

Zhang, J., Shi, F., Badour, K., Deng, Y., McGavin, M.K., and Siminovitch, K.A. (2002). WASp verprolin homology, cofilin homology, and acidic region domain-mediated actin polymerization is required for T cell development. Proc. Natl. Acad. Sci. USA *99*, 2240–2245.